ACS EARTH AND SPACE CHEMISTRY

http://pubs.acs.org/journal/aesccq

Article

Deliquescence Relative Humidity and Reversible Non-deliquescent Water Uptake in the Sodium Salts of Succinic Acid

Keith D. Beyer*

Cite This: https://doi.org/10.1021/acsearthspacechem.1c00168

Read Online

ACCESS | Metrics & More | Article Recommendations | Supporting Information

ABSTRACT: When metal ions from sea spray and other sources interact with dicarboxylic acids dissolved in atmospheric droplets, the results can be the precipitate of organic salts under dry atmospheric conditions. This study focused on the hygroscopic properties of the sodium salts of succinic acid ($NaHC_4H_4O_4$ and $Na_2C_4H_4O_4$). The salts reversibly take up water at relative humidities (RHs) lower than the deliquescence relative humidity (DRH) at 298 K. At higher RH values, a normal DRH is observed and temperature-dependent values were determined. The enhanced water content of otherwise dry particles may have an impact on heterogeneous chemistry on these particles as well as their optical properties.

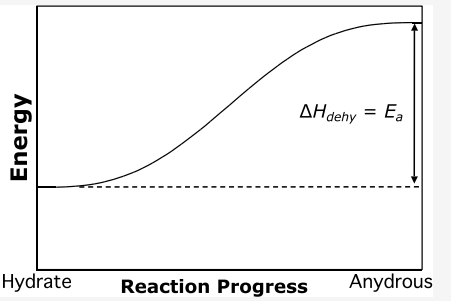

KEYWORDS: *sodium succinate, sodium hydrogen succinate, deliquescence, hygroscopicity, succinic acid*

INTRODUCTION

Aerosol−cloud interactions are a major area of uncertainty in climate studies, and chemical composition is a significant driver of cloud formation and cloud phase.[1,2] Field measurements of aerosols in the free and upper troposphere (UT) have shown that the major chemical components are sulfates, nitrates, ammonium, organic species, and mineral dust.[3,4] Among the organic components, dicarboxylic acids are present in aerosols in a range of environments, especially for aerosols that have undergone chemical aging.[5] Dicarboxylic acids are found in primary organic aerosols as well as secondary organic aerosols.[6] Field studies have shown an abundance of aerosols with organics and metals/metal salts from sea spray (Na and Mg),[5,7−9] biomass burning (K),[10,11] and mineral dusts/meteoritic material (Na, K, Ca, and Fe).[1,3,12−14] Field and lab studies have shown that metal ions can displace hydrogen ions from organic acids to form carboxylate salts in atmospheric aerosols.[7,9,15,16] For example, for a particle with dissolved NaCl and succinic acid that experienced UT temperatures and/or dry conditions, we would have

$$n\mathrm{NaCl(aq)} + \mathrm{H_2C_4H_4O_4(aq)} \rightarrow \mathrm{Na}_n\mathrm{H}_{2-n}\mathrm{C_4H_4O_4(s)} + n\mathrm{HCl(aq, g)} \quad (1)$$

where n equals 1 or 2. Studies have shown that the HCl product is highly volatile, leaving behind the organic salt in the particle.[9,15] Previous work has shown that sodium salts of succinic acid are much more soluble than succinic acid in water,[17] thus enhancing succinate ion concentrations in aqueous aerosols containing sodium ions, such as sea spray and continental aerosols. Recent field observations have shown that aerosols near the surface can be rapidly and efficiently transported to high altitudes in the UT via convective thunderstorms, which play a large role in the formation of cirrus clouds on synoptic and continental scales.[18−20] As the particles experience cold/dry conditions in the atmosphere, the sodium succinate salt could precipitate or contribute to glass formation of the aqueous phase of the aerosol.[16] However, there is very limited information in the literature regarding the hygroscopic properties of carboxylate salts. Peng and Chan used an electrodynamic balance (EDB) to study the hygroscopic properties of particles of several sodium carboxylates at 298 K, including sodium succinate.[21] Wu et al. used a hygroscopicity tandem differential mobility analyzer (H-TDMA) to study the hygroscopic properties of several sodium oxalates with and without ammonium sulfate present at 293 K; however, they only observed continuous water uptake in sodium succinate particles.[22] Thus, there are some challenges with the literature results for the deliquescence relative humidity (DRH) of sodium succinate, and there appear to be no studies on sodium hydrogen succinate DRH. Additionally, water uptake by "dry" particles has not been previously studied for either salt. This study presents quantitative observations of non-deliquescent water uptake by dried bulk powders of sodium succinate ($Na_2C_4H_4O_4$) and sodium hydrogen succinate ($NaHC_4H_4O_4$). The temperature-dependent DRH values for these powders after pre-DRH water absorption are also determined.

Special Issue: Mario Molina Memorial

Received: May 28, 2021
Revised: August 9, 2021
Accepted: August 11, 2021

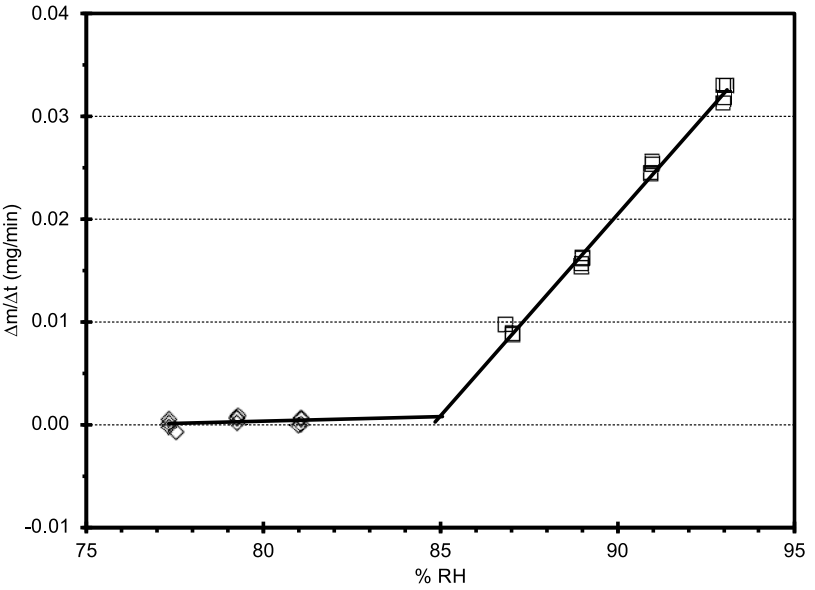

Figure 1. Change in mass over change in time ($\Delta m/\Delta t$) as a function of percent relative humidity (% RH) at 308.2 K for a dry $Na_2C_4H_4O_4$ sample with an initial mass of 2.871 mg. Solid lines are linear fits to the data before (◇) and after (□) the deliquescence point. The DRH is determined by simultaneously solving the two equations.

EXPERIMENTAL METHODS

Sample Preparation. Dry samples for analysis were made by preparing solutions with deionized water from chemical reagents: $H_2C_4H_4O_4$ (99% ACS reagent grade, Sigma-Aldrich) and NaOH (beads, Fisher). Solutions were made with 1:1 and 2:1 mole ratios of $NaOH/H_2C_4H_4O_4$ by completely dissolving solid reagents while stirring and gently heating. These solutions were made for solubility studies previously reported, and crystals that formed in these solutions but still in the mother liquor were analyzed via X-ray crystallography unit cell analysis.[17] The compounds were found to be $NaHC_4H_4O_4$ (1:1 $NaOH/H_2C_4H_4O_4$)[23] and $Na_2C_4H_4O_4{\cdot}6H_2O$ (2:1 $NaOH/H_2C_4H_4O_4$).[24] A portion of a high-concentration solution of each mole ratio was placed in a Petri dish at room temperature and open to air for drying. The measured lab room temperature averaged 295.5 K and 64% relative humidity (RH). The solvent evaporated, leaving only crystals after 24−48 h. The resulting crystals of each sample were then ground and stored in a desiccating cabinet for at least 2 months, during which time samples were not checked. When the ground crystals were visually inspected after 2 months using a microscope, $Na_2C_4H_4O_4{\cdot}6H_2O$ had changed in appearance from crystals to a dry powder with a very small fraction of single crystals. The $NaHC_4H_4O_4$ sample also appeared to be a powder with a small fraction of single crystals when inspected under a microscope. Further drying of the samples in a desiccating cabinet was an unexpected result and was not realized until DRH experiments were performed. Thus, the length of time needed to form "dry" samples was not determined nor was it a goal of this study.

Humidity-Controlled Thermogravimetric Analysis (HTGA). The experimental apparatus and methods used to determine water uptake and DRH with HTGA are described in detail in previous literature.[25] The main aspects of the experiments are outlined here. In thermogravimetric analysis (TGA), the mass of a sample is monitored to microgram accuracy as a function of the temperature. With HTGA, humidified air is introduced into the sample chamber at the sample. Experiments were performed on a Mettler-Toledo TGA/DSC1 coupled to a RH-200M humidity generator (VTI Corporation, now L&C Science and Technology). Humidified air can be supplied in the range of 2−95% RH at 278−353 K, with humidity control of ±1%. RH is measured with a dew point hygrometer with a measurement range of 233−333 K with an accuracy of ±0.2 K. To perform an experiment, a sample is placed in a 30 μL crucible made of platinum and inserted into the sample chamber along with an empty reference pan. Baseline noise for mass readings is typically on the order of 10 μg for a sample that is 0.5−6 mg. All experiments were conducted isothermally with the sample chamber temperature controlled by a circulator capable of achieving temperatures in the range of 233−473 K, with a temperature stability of ±0.02 K. The sample temperature reading of the HTGA instrument was calibrated with an Omega type T thermocouple (TMTSS-0326-12) connected to an Omega CSC32 readout. Both the thermocouple and readout were calibrated by Omega Engineering using instrumentation and standards traceable to the National Institute of Standards and Technology. Calibrated temperatures have an accuracy of ±0.3 K. All reported average experimental temperatures had a standard deviation of ±0.1 K or better.

To determine the DRH, the sample mass, heat flow, and RH were monitored simultaneously in an isothermal experiment as the RH was increased stepwise. Once RH has stabilized at each step, the $\Delta m/\Delta t$ (change in mass divided by the time interval between RH readings, 1 min in these experiments) is either 0 (pre-DRH) or a positive value (post-DRH). The uptake of water is accompanied by a flow of energy from the sample (exothermic) indicating that an energetic process is occurring, which is seen by an increase in heat flow values in the experiments. This heat flow signal is independent confirmation that an energetic process is occurring rather than instrument drift or other variation in the mass signal as a result of variation in the RH values. The raw data are then plotted as RH versus $\Delta m/\Delta t$, and each data set (pre- and post-DRH) is then fit separately to a linear equation, with these equations solved simultaneously to determine the DRH. An example plot of the data is given in Figure 1 for a DRH experiment involving $Na_2C_4H_4O_4$.

https://doi.org/10.1021/acsearthspacechem.1c00168
ACS Earth Space Chem. XXXX, XXX, XXX−XXX

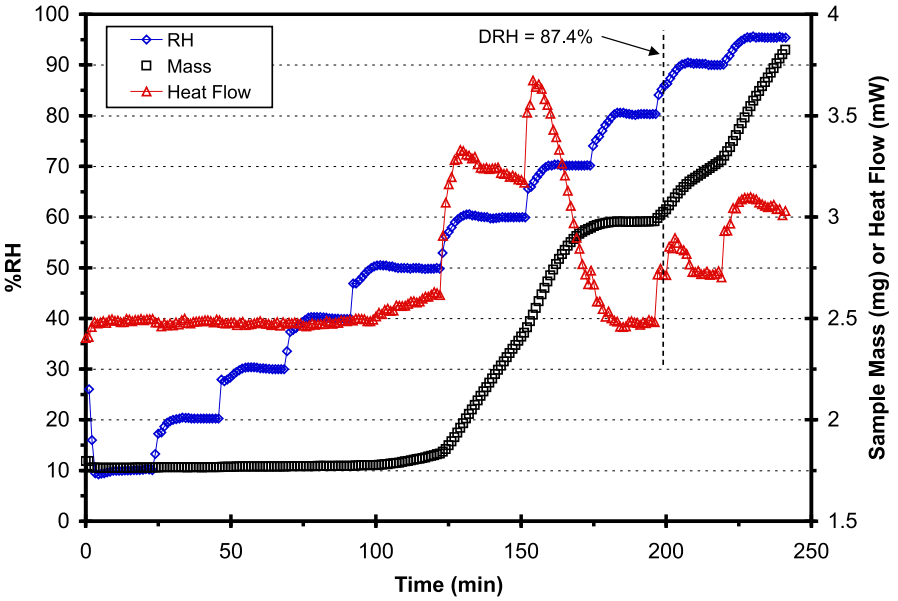

Figure 2. Mass and heat flow for a dry $Na_2C_4H_4O_4$ sample as a function of RH at 298.1 K from 10 to 95% RH. An increase in sample mass accompanied by heat from the sample (increase in heat flow) indicates water uptake by the sample. The DRH is indicated by the vertical line at 87.4% RH. Heat flow values shown in the figure are reduced by 3 mW from measured values to fit them on the same scale with sample mass.

Typically, data are collected at four RH values above and below the DRH (eight RH values total). Data at each RH are collected for 10 min (or 15 min for the first RH steps pre- and post-DRH to allow for additional equilibration time) once the measured RH values are consistent (typically within ±0.5% RH). In the subsequent analysis, the last four data measurements in each RH step are used to ensure that the most stable mass readings are used (constant air buoyancy).

Experiments involving pre-DRH water uptake by the samples were performed in a similar manner to the DRH experiments. However, in these experiments, the RH was kept below the DRH. As in the DRH experiments, the time clock for each step does not begin until the measured RH is consistent (although data are continually collected at 1 min intervals). In a typical experiment, a baseline mass was established for the sample by maintaining 40% RH for 10 min. Then, RH was increased stepwise to a suitable value below the DRH and held constant until water uptake completed (sample mass was constant, and there was no energy flow to or from the sample). RH was increased in either 10 or 15% RH increments to a maximum value below the DRH, where equilibrium was established (either 70% RH for $NaHC_4H_4O_4$ or 80% RH for $Na_2C_4H_4O_4$). The software algorithm controlling RH slightly overshoots the target RH values when moving from one step to another; therefore, the change in RH between each step was kept below 15%. Because the measured mass in the HTGA depends upon the buoyancy of air in the sample chamber, the RH was then reduced to 40% for 10 min to obtain the sample mass with the adsorbed water. RH was then decreased further to determine the point at which water was lost from the sample. The software settings for all HTGA experiments used the following convention: an increased heat flow signal (above the background level) corresponded to exothermic transitions, and decreased heat flow signals corresponded to endothermic transitions. In the experiments described here, water uptake by a sample was exothermic and water loss was endothermic, which is the case for most hydration/dehydration processes.[26]

The RH accuracy of these experiments was previously reported using compounds with a range of known DRH values and over a range of temperatures.[25] When experiments were performed in this study, the DRH of KCl and NaCl were checked periodically via experiments described above. These served as calibration standards, and the instrument was maintained within ±1% RH of the literature values for KCl and NaCl DRH at the experimental temperature.[27]

RESULTS

Pre-DRH Water Uptake. *$Na_2C_4H_4O_4$.* During the process of performing DRH experiments, pre-deliquescent water uptake by $Na_2C_4H_4O_4$ was observed. This is illustrated in Figure 2 for an experiment where humidity was stepped from 10 to 95% RH at 298.1 K. It is seen that the sample mass is constant up to 40% RH. At 50% RH, some water begins to be absorbed by the sample, as indicated by a slow increase in the sample mass and an increase in heat flow to the sample. In the steps to 60 and 70% RH, water is rapidly being taken up by the sample. However, this uptake ends at 80% RH: the sample mass levels off to a constant value, and heat flow returns to the pre-water uptake level. As a result of these observations for all samples at the temperatures studied, it became clear that the samples were absorbing water but not deliquescing below 80% RH. It should be noted that, when RH increased at each step in Figure 2, there is a very small increase in the measured sample mass whether water is being absorbed or not. These measured increases in sample mass (which are not accompanied by a change in heat flow) are due to a change in buoyancy of the chamber atmosphere at each RH step.[25]

Sodium succinate has a known hydrate: $Na_2C_4H_4O_4{\cdot}6H_2O$.[28] This hydrate was identified as the crystal forming in solutions in a previous study of the $Na_2C_4H_4O_4/H_2O$ phase diagram from this laboratory.[17] Therefore, an investigation was undertaken to determine whether this hydrate was forming in the DRH experiments as a result of water uptake by "dry" $Na_2C_4H_4O_4$ samples. In all cases, the dry powder $Na_2C_4H_4O_4$ was placed on the crucible bottom to form an approximately single layer.

https://doi.org/10.1021/acsearthspacechem.1c00168
ACS Earth Space Chem. XXXX, XXX, XXX−XXX

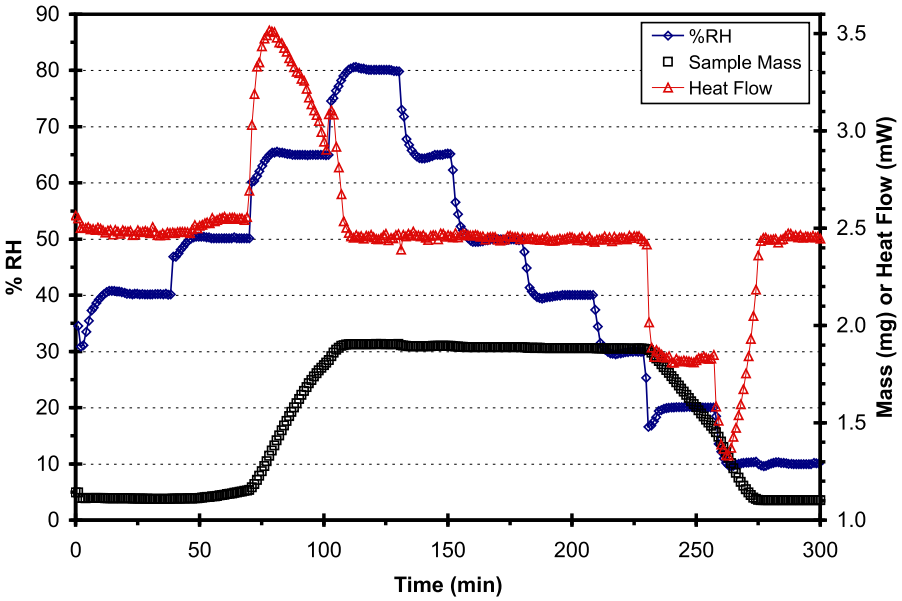

Figure 3. Mass and heat flow for a dry $Na_2C_4H_4O_4$ sample as a function of RH at 298.3 K. RH is stepped in increments as indicated by the blue diamonds and the left vertical axis, and sample mass and heat flow values are given on the right vertical axis. An increase in sample mass accompanied by an increase in heat flow from the sample (exothermic) indicates water uptake by the sample, while a decrease in sample mass accompanied by a decrease in heat flow from the sample (endothermic) indicates water loss by the sample. Heat flow values are reduced by 3 mW to plot sample mass and heat flow on the same scale.

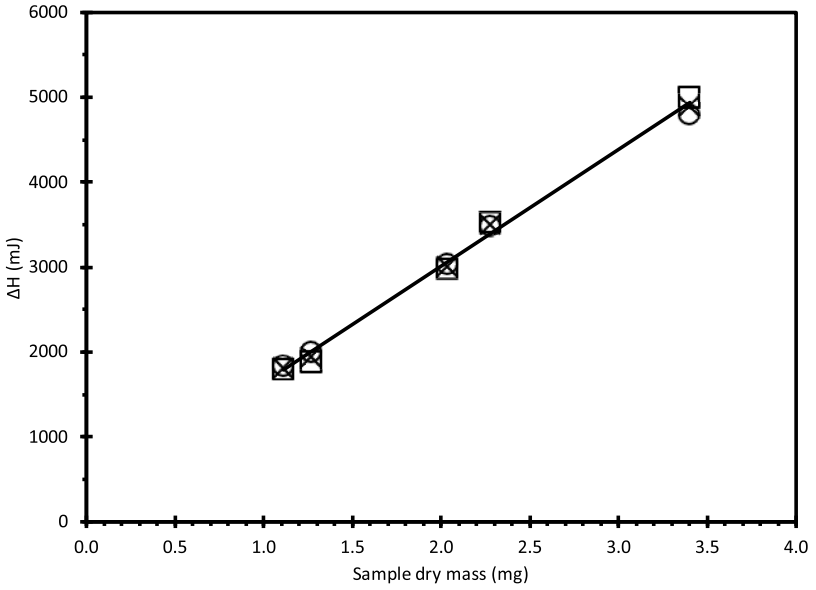

Figure 4. Enthalpy of water uptake and loss (presented as positive values) as a function of the dry sample mass (before water uptake) of $Na_2C_4H_4O_4$. Symbols are □, ΔH of water uptake; ○, ΔH of water loss; and ×, average enthalpy of water uptake and loss. The line is best fit through average ΔH values.

Experiments were performed where dry samples were held at 40% RH for 10 min to obtain an average sample mass at that RH. Then, RH was increased in steps to 80% for 30 min or longer to "saturate" the sample with water. The length of time was chosen to correspond with the sample mass (larger samples were held at 80% RH for longer times to ensure a constant mass was achieved, indicating that water uptake had completed). Humidity was then stepped down to 40% RH to obtain an accurate mass with the absorbed water. Then, the pre-water uptake mass at 40% RH (m_{dry}) and the post-water uptake mass also at 40% RH (m_{wet}) can be used to calculate the mass fraction (w) of $NaHC_4H_4O_4$ in the hydrated sample.

$$w = \frac{m_{dry}}{m_{wet}} \quad (2)$$

An example of this type of experiment is shown in Figure 3, where it is seen that water uptake begins at 50% RH and increases dramatically in the next step (65% RH). Water uptake completes in the 80% RH step, and the sample mass is then constant in the downward steps to 30% RH. With each step down in RH after the 80% RH step very slight decreases in the mass are observed at 65, 50, 40, and 30% RH as a result of a buoyancy change in the chamber atmosphere but no corresponding change in heat flow. Thus, no water was lost in

https://doi.org/10.1021/acsearthspacechem.1c00168
ACS Earth Space Chem. XXXX, XXX, XXX−XXX

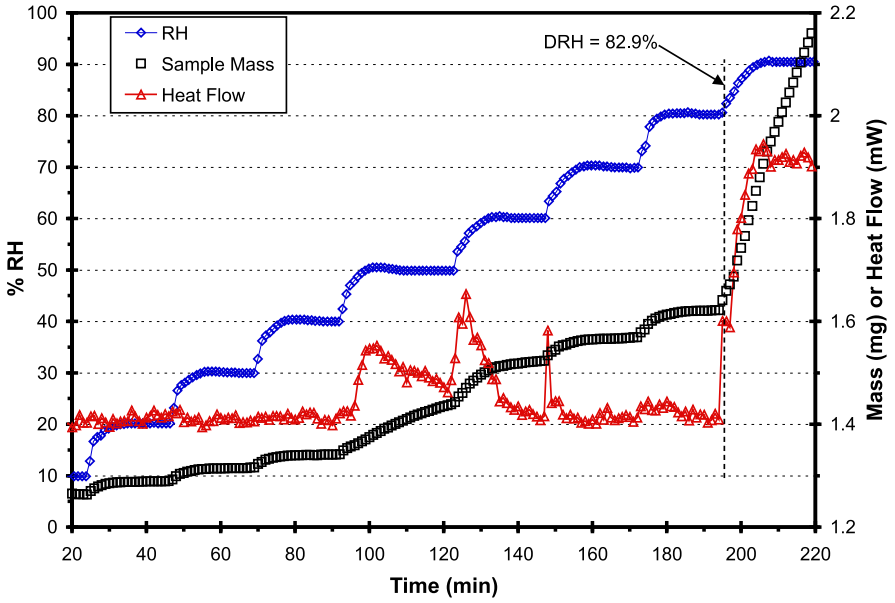

Figure 5. Mass and heat flow for a dry $NaHC_4H_4O_4$ sample as a function of RH at 298.1 K from 10 to 90% RH. An increase in sample mass accompanied by an increase in heat flow from the sample indicates water uptake by the sample. The DRH is indicated by the vertical line at 82.9% RH. Heat flow values shown in the figure are reduced by 4 mW from measured values to fit them on the same scale with the sample mass.

the RH steps down to 30% RH. Using the stable masses at 40% RH before and after water uptake, the mass fraction of $Na_2C_4H_4O_4$ can be calculated using eq 2. Eight experiments were performed at an average temperature of 298.2 K where this method was followed, and the average calculated mass fraction of $Na_2C_4H_4O_4$ after water uptake was $w = 0.596 \pm 0.005$. In comparison, $Na_2C_4H_4O_4{\cdot}6H_2O$ has a $Na_2C_4H_4O_4$ $w = 0.599$, and a saturated solution of $Na_2C_4H_4O_4$ at 298 K is $w = 0.259$.[17] The quantitative agreement between the calculated mass fraction of $Na_2C_4H_4O_4$ in the hydrated samples of these experiments and the composition of $Na_2C_4H_4O_4{\cdot}6H_2O$ provides strong evidence that hexahydrate is forming in the samples as a result of water uptake by the dry powder.

As shown in Figure 3, water uptake by $Na_2C_4H_4O_4$ is reversible. Once RH drops below 30%, a rapid decrease in sample mass ensues accompanied by a negative change in heat flow to the sample (endothermic). At 10% RH, the sample mass eventually stabilizes accompanied by a return to a constant heat flow at the background level, indicating that water loss by the sample has ended. Five experiments of this type were performed, and the heat flow signal was integrated for both water gain and loss. These ΔH values agreed to within ±3% or better. The two ΔH values were averaged (as positive values) and plotted as a function of the sample mass shown in Figure 4. A very good linear correlation between the dry sample mass and enthalpy is observed. Following the normal sign convention, endothermic values are positive (dehydration process) and exothermic values are negative (hydration process); therefore, the positive value of ΔH will be labeled "dehydration" (ΔH_{dehy}) for the remainder of this paper. The best fit line through the data is

$$\Delta H_{dehy} = 1375m + 263 \quad (3)$$

where ΔH_{dehy} is in millijoules and m is the dry mass of $Na_2C_4H_4O_4$ in milligrams. Theoretically, at zero mass, ΔH_{dehy} should be 0, and in comparison, eq 3 has a non-zero intercept. However, eq 3 is a fit to the average enthalpy values for hydration and dehydration in the experiments; thus, this introduces some uncertainty. Because the slope of the equation is large, extrapolation to zero mass would have significant uncertainty. The enthalpy values can be converted to molar values yielding an average $\Delta H_{dehy} = 248 \pm 12$ kJ/mol of $Na_2C_4H_4O_4$.

Further experiments were performed where RH was stepped in 1% RH increments to narrow the range where water uptake and loss are observed (three experiments each for water uptake and loss). At 298.2 K, water uptake occurs at 50.5 ± 0.7% RH and water loss occurs at 27.1 ± 0.7% RH.

$NaHC_4H_4O_4$. It was found that $NaHC_4H_4O_4$ water uptake follows a pattern similar to that observed for $Na_2C_4H_4O_4$. In the DRH experiments, it was again observed that water was being absorbed at RHs below the DRH. This is seen in Figure 5 for an experiment where humidity was stepped from 10 to 90% RH at 298.1 K. As seen in the figure, water uptake by the sample occurs as humidity is stepped from 40 to 50% RH. The water uptake is indicated by the sudden increase in mass and a change in heat flow from the sample. This occurs throughout the 50 and 60% RH steps, as indicated by a continual increase in mass of the sample and heat flow from the sample. There is even a slight increase in water uptake as humidity is increased from 60 to 70% RH (spike in heat flow). However, at 70% RH, the mass stabilizes and heat flow becomes constant. At this point, the sample appears to have "saturated" with respect to water. As RH is increased past 80%, mass again begins to increase, but this time, it is continuous and heat flow from the sample dramatically increases to a new constant value, indicating a thermal transition is occurring: deliquescence. As a result of these observations for all samples at the temperatures studied, it became clear that the samples were absorbing water but not deliquescing below 80% RH. As noted above, each RH step in Figure 5 is accompanied by a small increase in the measured sample mass as a result of a change in buoyancy of the chamber atmosphere.

Sodium hydrogen succinate has a known hydrate ($NaHC_4H_4O_4{\cdot}3H_2O$),[28] and an investigation was undertaken to determine whether this hydrate might be forming during non-deliquescence water uptake by the samples. As in the similar $Na_2C_4H_4O_4$ experiments, dry $NaHC_4H_4O_4$ was placed on the crucible bottom to form an approximately single layer.

https://doi.org/10.1021/acsearthspacechem.1c00168
ACS Earth Space Chem. XXXX, XXX, XXX−XXX

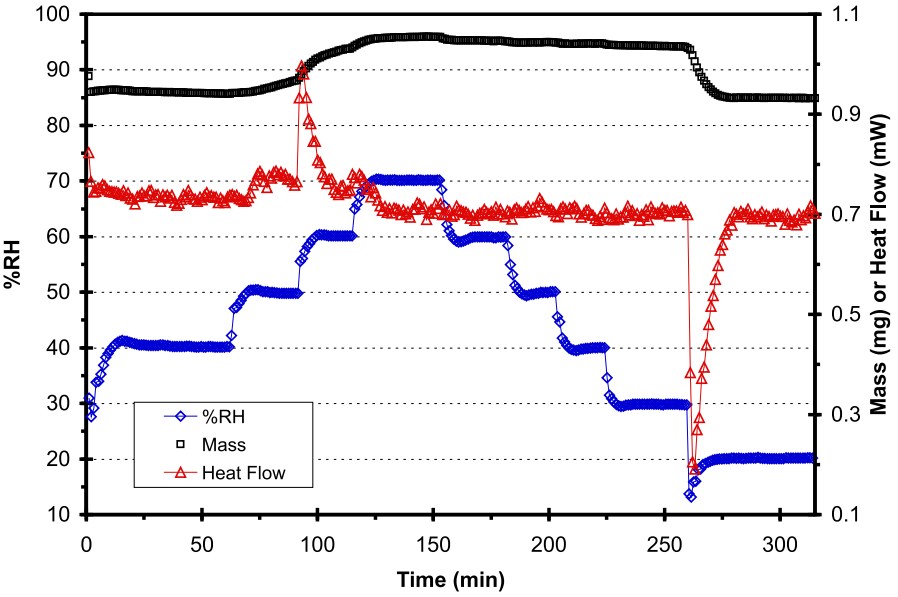

Figure 6. Mass and heat flow for a dry $NaHC_4H_4O_4$ sample as a function of RH at 298.2 K. RH is stepped in increments as indicated by the blue diamonds and the left vertical axis, and sample mass and heat flow values are given on the right vertical axis. An increase in sample mass accompanied by an increase in heat flow from the sample indicates water uptake by the sample, while a decrease in sample mass accompanied by a decrease in heat flow from the sample indicates water loss by the sample. Heat flow values shown in the figure are reduced by 4.8 mW from measured values to fit them on the same scale with the sample mass.

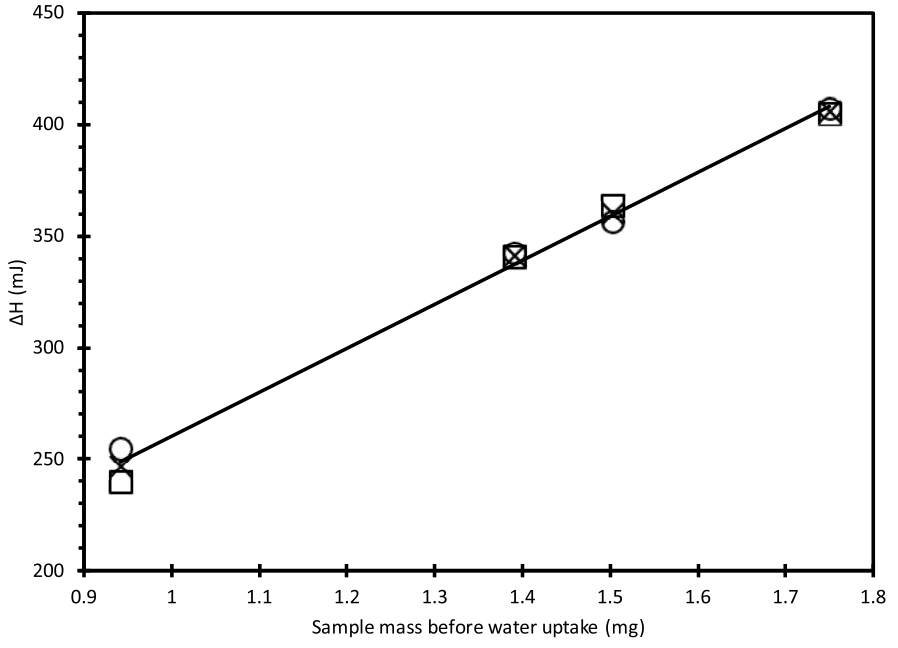

Figure 7. Enthalpy of water uptake and loss (as positive values) as a function of the dry sample mass (before water uptake) of $NaHC_4H_4O_4$. Symbols are □, ΔH of water uptake; ○, ΔH of water loss; and ×, average enthalpy of water uptake and loss. The line is best fit through average ΔH values.

Experiments were preformed where dry samples were held at 40% RH for 10 min to obtain an average sample mass at that RH. Then, RH was increased in steps to 70% for 30 min or longer to "saturate" the sample with water. The length of time was chosen to correspond with sample mass (larger samples were held at 70% RH for longer times to ensure a constant mass was achieved, indicating that water uptake had completed). Humidity was then stepped down to 40% RH to again obtain an accurate mass with the absorbed water. An example of this type of experiment is shown in Figure 6. Here, it is seen that once 70% RH is reached, the sample mass is stable and constant. With each step down in RH after the 70% RH step small decreases in the mass are observed at 60, 50, and 40% RH as a result of a buoyancy change in the chamber atmosphere but no corresponding change in heat flow. Thus, no water was lost in the RH steps down to 40% RH. Using the stable masses at 40% RH before and after water uptake, the mass fraction of $NaHC_4H_4O_4$ can be calculated using eq 2. Seven experiments were performed at an average temperature of 298.2 K where this method was followed, and an average calculated mass fraction of $NaHC_4H_4O_4$ after water uptake was $w = 0.909 \pm 0.010$. In comparison, $NaHC_4H_4O_4{\cdot}3H_2O$ has a $NaHC_4H_4O_4$ $w = 0.722$,

https://doi.org/10.1021/acsearthspacechem.1c00168
ACS Earth Space Chem. XXXX, XXX, XXX−XXX

and a saturated solution of $NaHC_4H_4O_4$ at 298 K is $w = 0.338$.[17] Thus, the hydrated samples had a water content significantly and consistently less than $NaHC_4H_4O_4·3H_2O$. This raises the question of another possible hydrate previously unreported. The composition of a hydrate with formula $NaHC_4H_4O_4·H_2O$ (sodium hydrogen succinate monohydrate) would be $w = 0.886$, while that of $NaHC_4H_4O_4·0.5H_2O$ would be $w = 0.940$. Clearly, the water content in the samples studied here is in between these values but slightly closer to the monohydrate. It seems likely that the "dry" $NaHC_4H_4O_4$ sample is not anhydrous, but rather trace amounts of water are present possibly forming $NaHC_4H_4O_4·H_2O$ before water uptake. It is unlikely that $NaHC_4H_4O_4·3H_2O$ is present in the samples, because single-crystal unit cell analysis from previous work indicated that the compound forming from solution was $NaHC_4H_4O_4$.[17] It is possible in the grinding process for the sample that some atmospheric water may have been absorbed by the sample that was not given up during drying.

As shown in Figure 6, water uptake by $NaHC_4H_4O_4$ is reversible. Once RH drops below 30%, a rapid decrease in sample mass ensues accompanied by a negative change in heat flow to the sample (endothermic). At 20% RH, the sample mass eventually stabilizes accompanied by a return to a constant heat flow at the background level, indicating that water loss by the sample has ended. Thus, $NaHC_4H_4O_4$ crystals will absorb water reversibly below the DRH in an isothermal environment. Four experiments of this type were performed, and the heat flow signal was integrated for both water gain and loss (as positive values). These ΔH values agreed to within ±3% or better. The two ΔH values were averaged and plotted as a function of the sample mass shown in Figure 7. A very good linear correlation between the dry sample mass and enthalpy is observed. The best fit line through the data is

$$\Delta H_{dehy} = 197.2m + 63.1 \quad (4)$$

where ΔH_{dehy} is in millijoules and m is the dry mass of $NaHC_4H_4O_4$ in milligrams. The enthalpy values can then be converted to molar values yielding an average $\Delta H_{dehy} = 34 \pm 2$ kJ/mol of $NaHC_4H_4O_4$. As with eq 3, it is noted that some uncertainty is inherent in eq 4, resulting in a non-zero y intercept.

Further experiments were also performed where RH was stepped in 1% RH increments to narrow the range where water uptake and loss are observed (three experiments each for water uptake and loss). At 298.2 K, it was determined that water uptake occurs at 51.8 ± 0.6% RH and water loss occurs at 25.9 ± 0.2% RH.

DELIQUESCENCE RELATIVE HUMIDITY (DRH)

DRH values of $Na_2C_4H_4O_4$ were determined at 288, 298, and 308 K, performing three (308 K) or four (298 and 288 K) experiments at each temperature. It is nearly certain that the crystals in the DRH experiments were $Na_2C_4H_4O_4·6H_2O$ after conditioning them at 80% RH for up to 40 min before RH was increased for DRH determination. The DRH results are given in Table 1 and shown in Figure 8. A linear fit to the data yields the temperature dependence (T in kelvin) of the DRH.

$$DRH = -0.220T + 153 \quad (5)$$

DRH as a fraction is equal to the water activity in a liquid sample. The solubility of $Na_2C_4H_4O_4·6H_2O$[28] has also been plotted in Figure 8, and it is seen that the mole fraction of water in a saturated solution is significantly different from its activity (DRH value as a fraction). Using these activities and the solubility data, activity coefficients for water can be determined

$$a_1 = \gamma_1 x_1 \quad (6)$$

where the subscript 1 indicates the solvent (water), a is the activity, γ is the activity coefficient, and x is the mole fraction. This equation was used to determine activity coefficients at each DRH temperature using a linear fit of the solubility data. These values are reported in Table 1, where it is seen that $Na_2C_4H_4O_4/H_2O$ solutions become less ideal as the temperature (and solute concentration) increases.

Table 1. DRH Values as a Function of the Temperature for $Na_2C_4H_4O_4·6H_2O$ and Water Activity Coefficients (γ) Determined from DRH Values and Solubility Data from Linke[28]

temperature (K)	sample mass (mg)	DRH	γ
308.2	3.421	85.3	0.892
308.3	4.224	85.6	0.895
308.2	2.871	85.0	0.890
298.4	5.160	87.3	0.907
298.4	3.992	87.3	0.907
298.4	0.927	87.4	0.908
288.5	3.080	89.3	0.921
288.3	1.500	89.5	0.924
288.4	7.531	90.1	0.930

DRH values of $NaHC_4H_4O_4$ samples at 288, 298, and 308 K were also determined, performing three experiments at each temperature. Given the water uptake phenomena described in the previous section, samples were held at 70% RH for up to 40 min to ensure that the sample mass stabilized before proceeding to higher RH values. Thus, the DRH values are for samples that are likely $NaHC_4H_4O_4·H_2O$ or a substantially similar composition. The results are given in Table 2 and shown in Figure 8. A linear fit to the data yields the temperature dependence (T in kelvin) of the DRH.

$$DRH = -0.341T + 185 \quad (7)$$

Thus, over this 20 K range, there is a strong temperature dependence, changing 7% RH. This dependence is greater than what was observed for $Na_2C_4H_4O_4·6H_2O$. As stated, the existence of the possible $NaHC_4H_4O_4·H_2O$ has not been previously reported; thus, solubility is unknown, and activity coefficients cannot be calculated.

DISCUSSION

A summary of the hygroscopic and thermal parameters measured in this study at 298 K is given in Table 3. In the literature, dehydration of crystal hydrates is commonly viewed as a reaction with activation energy (E_a) being a characteristic parameter reported.[26] For endothermic dehydration, the value of E_a must be at least as large as ΔH_{dehy}. Galwey and Brown[26] state that experimental E_a values for many reversible endothermic dehydrations are close to the respective ΔH_{dehy} values; thus, the value for ΔH of hydration and dehydration determined in the HTGA experiments may be viewed as a surrogate for dehydration E_a for purposes of comparison to the dehydration/hydration of other carboxylate salts. This is illustrated graphically in Figure 9. Dehydration is generally viewed as a nucleation/crystallization process: water is lost leaving behind an unstable "amorphous" structure. The more stable crystalline structure (which may be anhydrous or a lower

https://doi.org/10.1021/acsearthspacechem.1c00168
ACS Earth Space Chem. XXXX, XXX, XXX−XXX

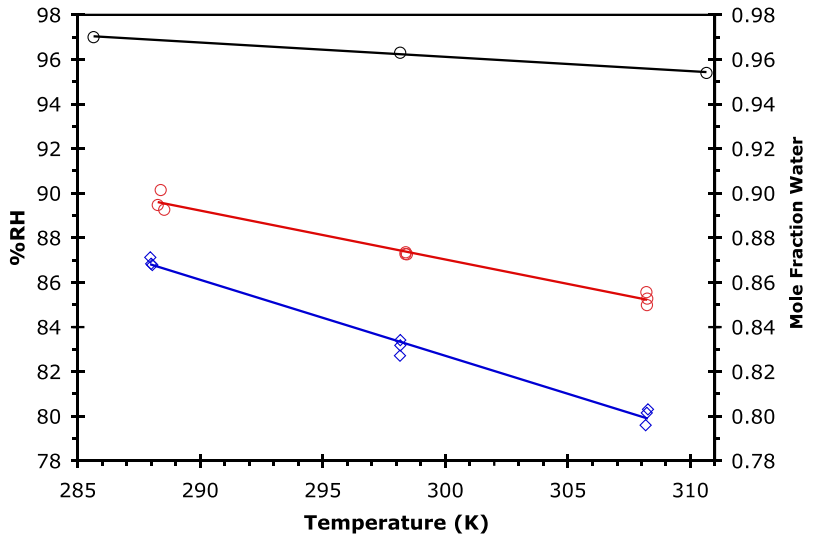

Figure 8. DRH values as a function of the temperature for $NaHC_4H_4O_4{\cdot}nH_2O$ (red circles) and $Na_2C_4H_4O_4{\cdot}6H_2O$ (blue diamonds) following the left vertical scale. Water mole fractions for saturated solutions of $Na_2C_4H_4O_4{\cdot}6H_2O$[28] are shown as black circles and follow the right vertical scale.

Table 2. DRH Values as a Function of the Temperature for $NaHC_4H_4O_4{\cdot}nH_2O$

temperature (K)	sample mass (mg)	DRH
308.2	8.107	79.6
308.3	7.776	80.3
308.2	8.134	80.2
298.1	2.247	82.7
298.2	3.881	83.4
298.2	4.414	83.2
288.0	5.240	87.1
288.0	5.055	86.8
288.0	3.915	86.8

hydrate) then nucleates and grows.[26,29] Hence, there is an energy barrier for the total dehydration process represented by the activation energy. Solid-state hydration is very important in pharmaceuticals, and Thukur and Thakuria published a review of this topic.[29] They state that organic compounds are highly susceptible to hydrate formation in the solid state, which agrees with the observation of Galwey and Brown[26] that, for many hydrations, $E_a = 0$,[26] as illustrated in Figure 9. However, hydrate formation is challenging to predict because water molecules easily incorporate into the crystal lattice and both thermodynamic and kinetic data are needed.[29]

With this background, it is noted that the value of ΔH_{dehy} for $Na_2C_4H_4O_4{\cdot}6H_2O$ (248 ± 12 kJ/mol) is in line with the value of E_a for dehydration of the polymorphs of $LiKC_4H_4O_6{\cdot}H_2O$ (range of 152−330 kJ/mol determined at 350−460 K)[30−32] and the dehydration of magnesium oxalate dihydrate ($MgC_2O_4{\cdot}2H_2O$, 111 kJ/mol determined at 425−500 K).[33] However, these E_a values are for dehydration at much higher temperatures than in the experiments in this study, and generally literature experiments are performed under vacuum or continuous dry gas

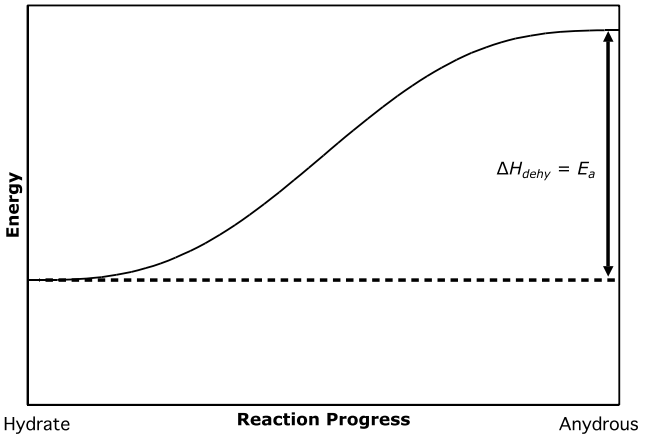

Figure 9. Graphical representation of the dehydration/hydration process. Dehydration is endothermic, while hydration is endothermic and typically with $E_a = 0$. Thus, ΔH_{dehy} is equal to E_a for dehydration for many hydrates.[26]

conditions.[26] If the enthalpy of dehydration for $Na_2C_4H_4O_4$ is viewed on a per water basis (248 kJ/6 waters of crystallization), the value of ΔH_{dehy} = 41 kJ/mol of water is just slightly lower than the enthalpy of vaporization of water (44.0 kJ/mol at 298 K[34]). Thus, water in $Na_2C_4H_4O_4{\cdot}6H_2O$ is likely lost at a rate similar to water evaporation at 298 K. For hydrates with more than one water, dehydration typically occurs in multiple steps with increasing energy required at each step.[35,36] However, no evidence was observed of partial dehydration of $Na_2C_4H_4O_4{\cdot}6H_2O$ in these experiments. Thus, there are multiple evidence that the hydrated water is weakly bound and readily dehydrates at atmospheric temperatures and pressures.

Table 3. Summary of Hygroscopic and Thermal Parameters Determined in This Study at 298 K

	dehydration RH	hydration RH	number of hydrated waters	DRH	ΔH_{dehy} (kJ/mol of salt)
$Na_2C_4H_4O_4$	27.1 ± 0.7	50.5 ± 0.7	6	87.3 ± 0.1	248 ± 12
$NaHC_4H_4O_4$	25.9 ± 0.2	51.8 ± 0.6	1[a]	83.1 ± 0.3	34 ± 2

[a]A precise stoichiometric value was not obtained. This value was the most plausible.

https://doi.org/10.1021/acsearthspacechem.1c00168
ACS Earth Space Chem. XXXX, XXX, XXX−XXX

For $NaHC_4H_4O_4{\cdot}H_2O$, ΔH_{dehy} (34.2 ± 2.2 kJ/mol) is well below the E_a value for the tartrate and oxalate hydrates mentioned and is below the enthalpy of vaporization of water (44.0 kJ/mol at 298 K[34]). Thus, the water appears to be very loosely bound in $NaHC_4H_4O_4{\cdot}H_2O$ and again may be lost at a rate similar to water evaporation at 298 K. The reversible water gain and loss from sodium salts of succinic acid appear novel when comparing to other sodium salts of dicarboxylic acids. Previous studies of the hygroscopic properties of several metal dicarboxylate hydrates ($NaHC_2O_4{\cdot}H_2O$, $NaHC_3H_2O_4{\cdot}H_2O$, and $Na_2C_4H_2O_4{\cdot}H_2O$) and non-metal carboxylate hydrate salts [$NH_4HC_2O_4{\cdot}0.5H_2O$ and $(NH_4)_2C_2H_4{\cdot}H_2O$] did not observe water loss or hydration below the DRH.[37] The total mass of the samples studied in the HTGA was larger than that expected in the atmosphere for dry particles. However, differences in mass would only affect the time required for complete hydration or dehydration of solids. Thus, atmospheric particles with smaller mass/sizes would be expected to complete the hydration/dehydration process more quickly than those observed here under the same RH and temperature conditions. Additionally, samples in this study were in contact with the surface of a platinum pan. However, there is no evidence in the literature this impacts either the hydration/dehydration process,[26] and DRH measurements for various atmospheric compounds in particle studies have been in good agreement with those determined with HTGA.[25,37]

With respect to DRH values, Wu et al.[22] studied the hygroscopic behavior of $Na_2C_4H_4O_4$ at 293 K using a H-TDMA. However, they only observed continuous water uptake of their dry particles (no DRH). The residence time in the humidifier was stated to be 2.5 s, which may not have been long enough to observe deliquescence; a limitation they recognized. Using eq 5, the calculated DRH at 293 K would be 88.7% RH. This value is at the limit of the RH values that they studied (their Figure 1d), and thus, it is reasonable that they did not observe the DRH. It is plausible that their observation of continuous water uptake was dry sodium succinate hydrating to form the hexahydrate, which did not complete in the short time of their experiment. In their Figure 1d, they show an increasing growth factor as water activity (RH) is increased. As RH increases, the rate of water uptake by $Na_2C_4H_4O_4$ increases, as seen in Figures 2 and 3 of this work. Thus, one would expect an increasing growth factor as RH increases if equilibrium has not been established.

Peng and Chan[21] studied the hygroscopic properties of sodium succinate using an EDB, reporting a crystallization relative humidity (CRH) and DRH at 298 K. Their results are based on drying and rehydrating two individual particles and show water loss of the particles between 46.7 and 47.9% RH (CRH) and DRH between 63.5 and 66% RH (one particle). From their reported values, the mass fraction of solute (mfs) appears to be ∼0.47 at the DRH (their Figure 7); however, this contradicts the solubility data and their bulk measurements where mfs = 0.259 for a solution saturated with $Na_2C_4H_4O_4{\cdot}6H_2O$. Peng and Chan suggest that this may indicate the existence of a lower hydrate; however, evidence for such a hydrate has not be reported elsewhere. In the water uptake experiments reported here for dry $Na_2C_4H_4O_4$, water uptake was observed at just under 51% RH. It is noted that Peng and Chan saw a roughly linear increase in water uptake at RH values above their reported DRH (63.5−66% RH), and the rate of uptake increased at RH values above the DRH reported here and seen in their bulk measurements (88.3%). Additionally, their CRH values correspond to mfs = ∼0.60 (their Figure 7), which equates to a $H_2O/Na_2C_4H_4O_4$ ratio of 6. Thus, their "CRH" may have been dehydration of $Na_2C_4H_4O_4{\cdot}6H_2O$. Finally, it is observed that at least one particle in the experiments of Peng and Chan appears to have been exposed to RH < 30%; however, no change in mass was observed in their experiment, further indicating that the particle may have been anhydrous rather than hexahydrate. Taking these observations into account, it seems possible that they were observing effects similar to those reported here as a result of dehydrating and hydrating of $Na_2C_4H_4O_4{\cdot}6H_2O/Na_2C_4H_4O_4$, although at higher RH values (∼15% RH higher).

SUMMARY AND CONCLUSION

Reversible non-deliquescent water uptake was observed at 298 K and atmospheric pressure for the single and double sodium salts of succinic acid, as summarized in Table 3. The enthalpies of the water loss and uptake were nearly identical for each respective salt, and on a per water basis, the enthalpies were less than that for water vaporization at 298 K. For $NaHC_4H_4O_4$, experimental evidence points to formation of a previously unreported monohydrate. For $Na_2C_4H_4O_4$, the formation of the known hexahydrate quantitatively matches the amount of water absorbed. The reversible behavior at 298 K seems to be unusual because there are no reports for similar compounds in the literature,[26] and studies on other sodium salts of oxalates and malonates did not observe pre-deliquescent water uptake.[37] In addition, temperature-dependent DRH values for the sodium salts of succinic acid have been investigated, and activity coefficients of water have been determined for solutions saturated with $Na_2C_4H_4O_4{\cdot}6H_2O$, where it is found that saturated solutions become less ideal as the temperature and solute concentration increases. The DRH values are in the same range as those reported for other sodium salts of dicarboxylic acids.[37] The hygroscopic behavior of sodium succinate in previous lab studies reported in the literature could be interpreted as hydration and dehydration processes rather than deliquescence/efflorescence[21] or lack thereof.[22]

The particulate water content has strong implications for heterogeneous reaction rates and radiative properties of atmospheric particles.[38] The results reported here have shown that dry particles containing sodium and succinate will take up and lose water below the respective DRH values. Thus, even "dry" particles may still have water content as a hydrate, but the hydrated water may be readily lost at very low RHs. Existence of hydrates in otherwise dry particles may affect their optical properties and will affect their surface properties because the hydrated crystal structure is nearly always different from the dehydrated structure.[39,40] These two effects have implications for particle surface chemistry and Earth's radiation balance. In addition, the sodium salts of succinic acid are much more soluble than succinic acid;[17] thus, succinate ions will persist in solution containing sodium ions at concentrations higher than in the absence of sodium. Therefore, the quantity of sodium salts of succinic acid will be enhanced in aerosols with a sodium ion content, such as sea spray and continental aerosols.

ASSOCIATED CONTENT

Supporting Information

The Supporting Information is available free of charge at https://pubs.acs.org/doi/10.1021/acsearthspacechem.1c00168.

https://doi.org/10.1021/acsearthspacechem.1c00168
ACS Earth Space Chem. XXXX, XXX, XXX−XXX

Alternate plots of Figures 2, 3, 5, and 6 with RH as the *x*-axis variable (Figures S1−S4) (PDF)

AUTHOR INFORMATION

Corresponding Author

Keith D. Beyer − *Department of Chemistry and Biochemistry, University of Wisconsin—La Crosse, La Crosse, Wisconsin 54601, United States;* orcid.org/0000-0003-0630-7575; Email: kbeyer@uwlax.edu

Complete contact information is available at: https://pubs.acs.org/10.1021/acsearthspacechem.1c00168

Notes

The author declares no competing financial interest.

ACKNOWLEDGMENTS

This research was supported by the National Science Foundation (Alexandria, VA, U.S.A.) Atmospheric Chemistry Program (AGS-1361592). The author thanks Drs. Ilia Guzei, Kendric Nelson, and Robert McGaff for helpful discussions regarding crystal composition and Lucas Buttke for running some of the DRH experiments.

REFERENCES

(1) Cziczo, D. J.; Froyd, K. D.; Hoose, C.; Jensen, E. J.; Diao, M.; Zondlo, M. A.; Smith, J. B.; Twohy, C. H.; Murphy, D. M. Clarifying the Dominant Sources and Mechanisms of Cirrus Cloud Formation. *Science* **2013**, *340* (6138), 1320−1324.

(2) DeMott, P. J.; Prenni, A. J.; Liu, X.; Kreidenweis, S. M.; Petters, M. D.; Twohy, C. H.; Richardson, M. S.; Eidhammer, T.; Rogers, D. C. Predicting Global Atmospheric Ice Nuclei Distributions and Their Impacts on Climate. *Proc. Natl. Acad. Sci. U. S. A.* **2010**, *107* (25), 11217−11222.

(3) Murphy, D. M.; Thomson, D. S.; Mahoney, T. M. J. In Situ Measurements of Organics, Meteoritic Material, Mercury, and Other Elements in Aerosols at 5 to 19 Kilometers. *Science* **1998**, *282*, 1664−1669.

(4) Froyd, K. D.; Murphy, D. M.; Lawson, P.; Baumgardner, D.; Herman, R. L. Aerosols That Form Subvisible Cirrus at the Tropical Tropopause. *Atmos. Chem. Phys.* **2010**, *10* (1), 209−218.

(5) Sullivan, R. C.; Prather, K. A. Investigations of the Diurnal Cycle and Mixing State of Oxalic Acid in Individual Particles in Asian Aerosol Outflow. *Environ. Sci. Technol.* **2007**, *41* (23), 8062−8069.

(6) Seinfeld, J. H.; Pandis, S. N. *Atmospheric Chemistry and Physics: From Air Pollution to Climate Change*; Wiley: New York, 1998.

(7) Kerminen, V.-M.; Teinilä, K.; Hillamo, R.; Pakkanen, T. Substitution of Chloride in Sea-Salt Particles by Inorganic and Organic Anions. *J. Aerosol Sci.* **1998**, *29* (8), 929−942.

(8) Kojima, T.; Buseck, P. R.; Iwasaka, Y.; Matsuki, A.; Trochkine, D. Sulfate-Coated Dust Particles in the Free Troposphere over Japan. *Atmos. Res.* **2006**, *82* (3−4), 698−708.

(9) Laskin, A.; Moffet, R. C.; Gilles, M. K.; Fast, J. D.; Zaveri, R. A.; Wang, B.; Nigge, P.; Shutthanandan, J. Tropospheric Chemistry of Internally Mixed Sea Salt and Organic Particles: Surprising Reactivity of NaCl with Weak Organic Acids. *J. Geophys. Res.: Atmos.* **2012**, *117* (D15), D15302.

(10) Reid, J. S.; Koppmann, R.; Eck, T. F.; Eleuterio, D. P. A Review of Biomass Burning Emissions Part II: Intensive Physical Properties of Biomass Burning Particles. *Atmos. Chem. Phys.* **2005**, *5* (3), 799−825.

(11) Zauscher, M. D.; Wang, Y.; Moore, M. J. K.; Gaston, C. J.; Prather, K. A. Air Quality Impact and Physicochemical Aging of Biomass Burning Aerosols during the 2007 San Diego Wildfires. *Environ. Sci. Technol.* **2013**, *47* (14), 7633−7643.

(12) Hinz, K.-P.; Trimborn, A.; Weingartner, E.; Henning, S.; Baltensperger, U.; Spengler, B. Aerosol Single Particle Composition at the Jungfraujoch. *J. Aerosol Sci.* **2005**, *36* (1), 123−145.

(13) Murphy, D. M.; Cziczo, D. J.; Froyd, K. D.; Hudson, P. K.; Matthew, B. M.; Middlebrook, A. M.; Peltier, R. E.; Sullivan, A.; Thomson, D. S.; Weber, R. J. Single-Particle Mass Spectrometry of Tropospheric Aerosol Particles. *J. Geophys. Res.: Atmos.* **2006**, *111* (D23), D23S32.

(14) Sullivan, R. C.; Guazzotti, S. A.; Sodeman, D. A.; Prather, K. A. Direct Observations of the Atmospheric Processing of Asian Mineral Dust. *Atmos. Chem. Phys.* **2007**, *7* (5), 1213−1236.

(15) Ghorai, S.; Wang, B.; Tivanski, A.; Laskin, A. Hygroscopic Properties of Internally Mixed Particles Composed of NaCl and Water-Soluble Organic Acids. *Environ. Sci. Technol.* **2014**, *48* (4), 2234−2241.

(16) Wang, B.; O'Brien, R. E.; Kelly, S. T.; Shilling, J. E.; Moffet, R. C.; Gilles, M. K.; Laskin, A. Reactivity of Liquid and Semisolid Secondary Organic Carbon with Chloride and Nitrate in Atmospheric Aerosols. *J. Phys. Chem. A* **2015**, *119* (19), 4498−4508.

(17) Beyer, K. D.; Buttke, L. G. Solubilities in Aqueous Solutions of the Sodium Salts of Succinic and Glutaric Acid with and without Ammonium Sulfate. *J. Chem. Thermodyn.* **2018**, *125*, 189−199.

(18) Corr, C. A.; Ziemba, L. D.; Scheuer, E.; Anderson, B. E.; Beyersdorf, A. J.; Chen, G.; Crosbie, E.; Moore, R. H.; Shook, M.; Thornhill, K. L.; Winstead, E.; Lawson, R. P.; Barth, M. C.; Schroeder, J. R.; Blake, D. R.; Dibb, J. E. Observational Evidence for the Convective Transport of Dust over the Central United States. *J. Geophys. Res.: Atmos.* **2016**, *121* (3), 1306−1319.

(19) Twohy, C. H.; Clement, C. F.; Gandrud, B. W.; Weinheimer, A. J.; Campos, T. L.; Baumgardner, D.; Brune, W. H.; Faloona, I.; Sachse, G. W.; Vay, S. A.; Tan, D. Deep Convection as a Source of New Particles in the Midlatitude Upper Troposphere. *J. Geophys. Res.: Atmos.* **2002**, *107* (D21), AAC 6-1−AAC 6-10.

(20) Cui, Z.; Carslaw, K. S. Enhanced Vertical Transport Efficiency of Aerosol in Convective Clouds Due to Increases in Tropospheric Aerosol Abundance. *J. Geophys. Res.: Atmos.* **2006**, *111* (D15), D15212.

(21) Peng, C.; Chan, C. K. The Water Cycles of Water-Soluble Organic Salts of Atmospheric Importance. *Atmos. Environ.* **2001**, *35* (7), 1183−1192.

(22) Wu, Z. J.; Nowak, A.; Poulain, L.; Herrmann, H.; Wiedensohler, A. Hygroscopic Behavior of Atmospherically Relevant Water-Soluble Carboxylic Salts and Their Influence on the Water Uptake of Ammonium Sulfate. *Atmos. Chem. Phys.* **2011**, *11* (24), 12617−12626.

(23) Mallinson, P. R.; Frampton, C. S. Structure of Sodium Hydrogen Succinate at 123 K. *Acta Crystallogr., Sect. C: Cryst. Struct. Commun.* **1992**, *48* (8), 1555−1556.

(24) Fonseca, I.; Martínez-Carrera, S.; García-Blanco, S. Structure of Sodium Succinate Hexahydrate. *Acta Crystallogr., Sect. C: Cryst. Struct. Commun.* **1986**, *42* (9), 1123−1125.

(25) Beyer, K. D.; Schroeder, J. R.; Kissinger, J. A. Temperature-Dependent Deliquescence Relative Humidities and Water Activities Using Humidity Controlled Thermogravimetric Analysis with Application to Malonic Acid. *J. Phys. Chem. A* **2014**, *118* (13), 2488−2497.

(26) Galwey, A. K.; Brown, M. E. *Thermal Decomposition of Ionic Solids: Studies in Physical and Theoretical Chemistry*; Elsevier: Amsterdam, Netherlands, 1999.

(27) Greenspan, L. Humidity Fixed Points of Binary Saturated Aqueous Solutions. *J. Res. Natl. Bur. Stand., Sect. A* **1977**, *81A*, 89−96.

(28) Linke, W. F. *Solubilities: Inorganic and Metal Organic Compounds: A Revision and Continuation of the Compilation by A. Seidell*, 4th ed.; Van Nostrand: New York, 1958.

(29) Thakur, T. S.; Thakuria, R. Crystalline Multicomponent Solids: An Alternative for Addressing the Hygroscopicity Issue in Pharmaceutical Materials | Crystal Growth & Design. *Cryst. Growth Des.* **2020**, *20* (9), 6245−6265.

(30) Bhattamisra, S. D.; Laverty, G. M.; Baranov, N. A.; Okhotnikov, V. B.; Galwey, A. K. The Kinetics and Mechanism of Water Evolution from Molten *dl* Lithium Potassium Tartrate Monohydrate. *Philos. Trans. R. Soc., A* **1992**, *341* (1662), 479−498.

(31) Galwey, A. K.; Laverty, G. M.; Okhotnikov, V. B.; O'Neill, J. A Kinetic Study of Water Evolution from a Molten Hydrated Salt. *J. Therm. Anal.* **1992**, *38* (3), 421−428.

(32) Galwey, A. K.; Laverty, G. M.; Baranov, N. A.; Okhotnikov, V. B. The Solid State Dehydration of *d* Lithium Potassium Tartrate Monohydrate Is Complete in Two Rate Processes II. The Nucleation and Growth Second Reaction and Dehydration Mechanism. *Philos. Trans. R. Soc., A* **1994**, *347* (1682), 157−184.
(33) Masuda, Y.; Iwata, K.; Ito, R.; Ito, Y. Kinetics of the Thermal Dehydration of Magnesium Oxalate Dihydrate in a Flowing Atmosphere of Dry Nitrogen. *J. Phys. Chem.* **1987**, *91* (26), 6543−6547.
(34) *Lange's Handbook of Chemistry*, 14th ed.; Dean, J. A., Ed.; McGraw-Hill: New York, 1992.
(35) Topley, B. The Mechanism and Molecular Statistics of the Reaction $CuSO_4 \cdot 5H_2O = CuSO_4 \cdot H_2O + 4H_2O$. *Philos. Trans. R. Soc., A* **1932**, *136* (829), 413−428.
(36) *Reactivity of Solids: Proceedings of the Seventh International Symposium on the Reactivity of Solids, Bristol, 17−21 July 1972*; Anderson, J. S., Roberts, M. W., Stone, F. S., Eds.; Chapman and Hall: London, U.K., 1972.
(37) Schroeder, J. R.; Beyer, K. D. Deliquescence Relative Humidities of Organic and Inorganic Salts Important in the Atmosphere. *J. Phys. Chem. A* **2016**, *120* (50), 9948−9957.
(38) Seinfeld, J. H.; Pandis, S. N. *Atmospheric Chemistry and Physics: From Air Pollution to Climate Change*, 2nd ed.; John Wiley & Sons: Hoboken, NJ, 2006.
(39) Garner, W. E. *Chemistry of the Solid State*; Academic Press: New York, 1955.
(40) Dell, R. M.; Wheeler, V. J. In *Reactivity of Solids: 5th International Symposium on the Reactivity of Solids*; Schwab, G. M., Ed.; Elsevier: Amsterdam, Netherlands, 1965; p 694.

https://doi.org/10.1021/acsearthspacechem.1c00168
ACS Earth Space Chem. XXXX, XXX, XXX−XXX